ADVANCED SUSTAINABLE SYSTEMS
www.advsustainsys.com

# Sustainable Flame-Retardant Poly Lactic Acid Biocomposites Reinforced with Polyphosphate-Enriched Microalgae: Unlocking the Potential of Hyper-Compensation

*Rohit Dey,* Mateusz Dudziak, Andreas Prescher, Timmu Kreitsmann, Keran Zhang, Clemens Posten, Claudia Thomsen, Bernhard Schartel, Matthias S. Ullrich, and Laurenz Thomsen*

**This study examines the dual benefits of microalgae cultivation for wastewater treatment and the enhancement of polylactic acid-based biocomposites. Using Desmodesmus sp. in a photobioreactor, both batch and continuous operations achieve total nitrogen (TN) and total phosphorus (TP) removal rates of up to 99.9%, maintaining TN and TP levels below 0.02 mg $L^{-1}$ in the effluent, aligning with European discharge standards. Continuous cultivation increases biomass productivity from 0.102 to 0.43 g $L^{-1}$ $day^{-1}$, a 322% improvement over batch operations. Nutrient starvation followed by reintroduction to nutrient-rich wastewater induces hyper-compensation luxury uptake, with P-enriched cells accumulating 1.33% intracellular P within six hours — 21% higher than natural accumulation. The results reveal that luxury phosphorus uptake in microalgae follows a triphasic system of uptake and storage, challenging the previously suggested biphasic model. When incorporated into Poly lactic acid (PLA), the biomass enhances versatility, offering potential replacement of inorganic P in industrial applications, particularly flame retardants. Pyrolysis and cone calorimetry confirm the thermal and fire-retardant benefits, with a 20% reduction in peak heat release rate and increased char yield. This work highlights microalgae's role in sustainable biocomposites, supporting wastewater treatment, nutrient recovery, and $CO_2$ sequestration.**

## 1. Introduction

The increasing significance of using renewable raw materials for plastic production has been evident in recent years. Thermoplastic polymers, such as polylactides (PLA), polyhydroxyalkanoates (PHA), and thermoplastic starch (TPS), derived from renewable sources, require carefully designed material compositions to improve product performance, equaling petroleum-based polymers.[1] One critical property for technical polymers used in fields like electrical engineering, construction, and transport is flame retardancy.[2] To reduce environmental impacts and ensure sustainability, the production of bio-based materials must undergo further optimization.[3] However, adding processing, durability, and material property enhancers can pose environmental challenges. For example, flame retardants (FR) and Flame Stable Materials (FSMs) can have significant environmental drawbacks. Although halogen-free, phosphorus-containing FSMs are currently the industry standard and are often touted as "environmentally friendly," this label is frequently applied without adequate justification. Such FSMs still fall short of the requirements for a sustainable recycling economy in terms of raw material sources and processing methods.[2] Environmental concerns have driven research to find alternatives to halogen-containing FSMs, resulting in renewed interest in phosphorus (P) and its recovery. The primary goal of the current project is to replace non-renewable

R. Dey, A. Prescher, T. Kreitsmann, K. Zhang, M. S. Ullrich, L. Thomsen
School of Science
Constructor University Bremen
Campus Ring 6, 28759 Bremen, Germany
E-mail: rdey@constructor.university

The ORCID identification number(s) for the author(s) of this article can be found under https://doi.org/10.1002/adsu.202500251



**DOI: 10.1002/adsu.202500251**

M. Dudziak, B. Schartel
Bundesanstalt für Materialforschung und -prüfunnter (BAM)
Unter den Eichen 87, 12205 Berlin, Germany

C. Posten
Institute of Life Science Engineering
Karlsruhe Institute of Technology
Fritz-Haber-Weg 2, 76131 Karlsruhe, Germany

C. Thomsen
iSeaMC GmbH
Campus Ring 1, 28759 Bremen, Germany

L. Thomsen
Department of Marine Sciences
University of Gothenburg
Göteborg 40530, Sweden

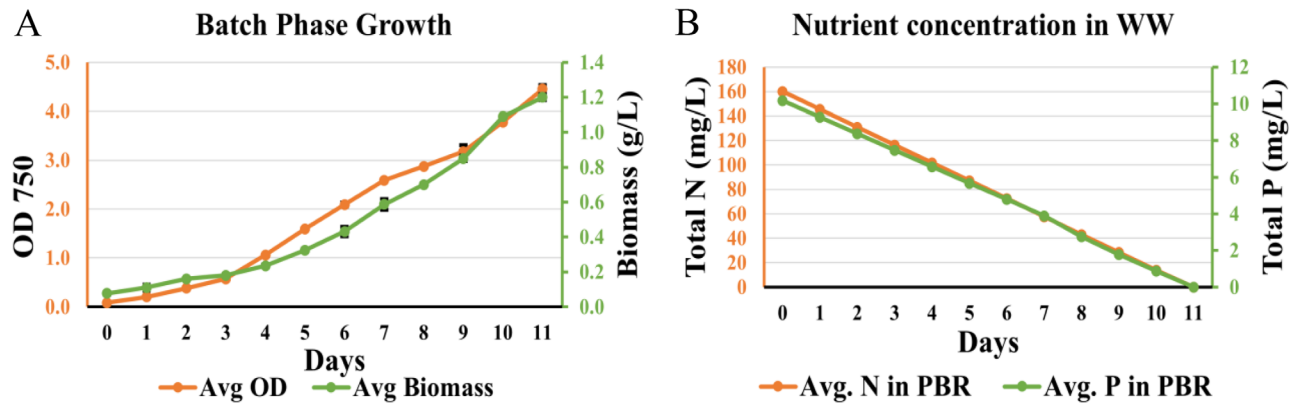


**Figure 1.** A) Growth kinetics of *Desmodesmus* sp. in the pilot plant. Average biomass and optical density monitored from 3 ($n = 3$) different locations of the photobioreactor system recorded at the same time daily. Error bars indicate the standard deviation. B) Nutrient levels measured in the photobioreactor during daily monitoring.

phosphate sources with a sustainable strategy for inorganic phosphorus recovery within a value-added cycle. The proposed solution involves developing a fully bio-based additive that ensures flame retardancy in bioplastics like PLA (biocomposite) while promoting a sustainable materials cycle.

Phosphorus plays a central role in flame protection, not only through a potential flame poisoning effect by forming P radicals (PO-) that react with fire-promoting hydrogen and hydroxyl radicals in the gas phase but also through the catalytic effect of P compounds (POH) in forming a char layer. This reduces the chain reactions responsible for flame propagation, effectively quenching the flame.[4] However, the raw material situation for inorganic P is problematic, as is the case for other applications of this essential element. Currently, the state-of-the-art phosphorus-containing FSMs, such as ammonium polyphosphate (APP) or aryl phosphates, are derived from non-renewable inorganic phosphate from phosphate mines, which is considered a critical raw material by the European Commission.[5,6] Although much research has been conducted on phosphorus recovery using microalgae, the recovered phosphorus is unusable is in the form of phospholipids and other DNA. The proposed project aims at using microalgae to recover P as acid insoluble inorganic poly phosphate bodies (PPB). This is the form of phosphorus that the microalgae quickly pack inorganic phosphorus into during luxury phosphorus uptake and only later slowly incorporates it into the cell.[7]

Optimizing nutrient recovery in wastewater treatment plants (WWTPs) is crucial to the value-creation system. Since October 2017, with the enactment of the new Sewage Sludge Ordinance, cities and municipalities in Germany have been required to incorporate phosphorus recycling into their wastewater treatment plants by 2032; with similar objectives being adopted globally.[8] One promising approach in this context is the use of microalgae.[9] While traditional methods of phosphorus recovery from sewage sludge involve complex post-treatment processes, utilizing native algae biomass simplifies this by only requiring phosphorus enrichment.[10] Importantly, this method might even enable the direct functional application of nutrient-enriched biomass. In addition to using microalgae from WWTPs as fertilizer, optimizing them for use as flame retardants (FSM) offers another promising avenue for a sustainable value-added cycle. The herein reported project aimed to demonstrate the production of a fully bio-based material system with integrated flame protection and test it in a prototype. Successfully implementing this bio-based process solution would contribute to establishing a new aquatic-based, sustainable value chain. To assess the effectiveness of microalgae in conventional polymer matrices, a benchmark polylactic acid (PLA) composite will be produced and tested. Thus, providing phosphorus-enriched microalgae from waste-water (WW), optimized for use as FR in thermoplastic bioplastics would enhance the position of any nation as a leading innovator in resource recovery and bioeconomy.

Previous studies have demonstrated that microalgae enriched with inorganic phosphorus (P) can enhance the properties of PLA biocomposites, particularly in flame retardancy.[11] Different weight percentages of the biomass was compounded into PLA biocomposites and tested for various physical, mechanical and chemical properties and compared against other biocomposites

**Table 1.** Biomass productivity, specific growth rate, and wastewater treatment efficiency.

| | Average Light Intensity ($\mu E\ m^{-2}\ s^{-1}$) | Mean specific growth rate ($\mu$) | Average N removal rate ($mg\ L^{-1}\ d^{-1}$) ($P_x$) | Average P removal rate ($mg\ L^{-1}\ d^{-1}$) ($P_x$) | WW purification rate ($L\ d^{-1}$) ($P_w$) | Biomass productivity ($g\ L^{-1}\ d^{-1}$) ($P_b$) |
|---|---|---|---|---|---|---|
| Batch Phase 1000 L | 456 | 0.25 | 14.54 | 0.91 | 91 | 0.102 |
| Continuous Phase | 320–800 | 0.25–0.40 | 37.50–60 | 2.50–4 | 250–400 | $0.43 \pm 0.10$ |
| % Improvement | | Upto 60% | 158–313 | 175–309 | 175–340 | 322 |

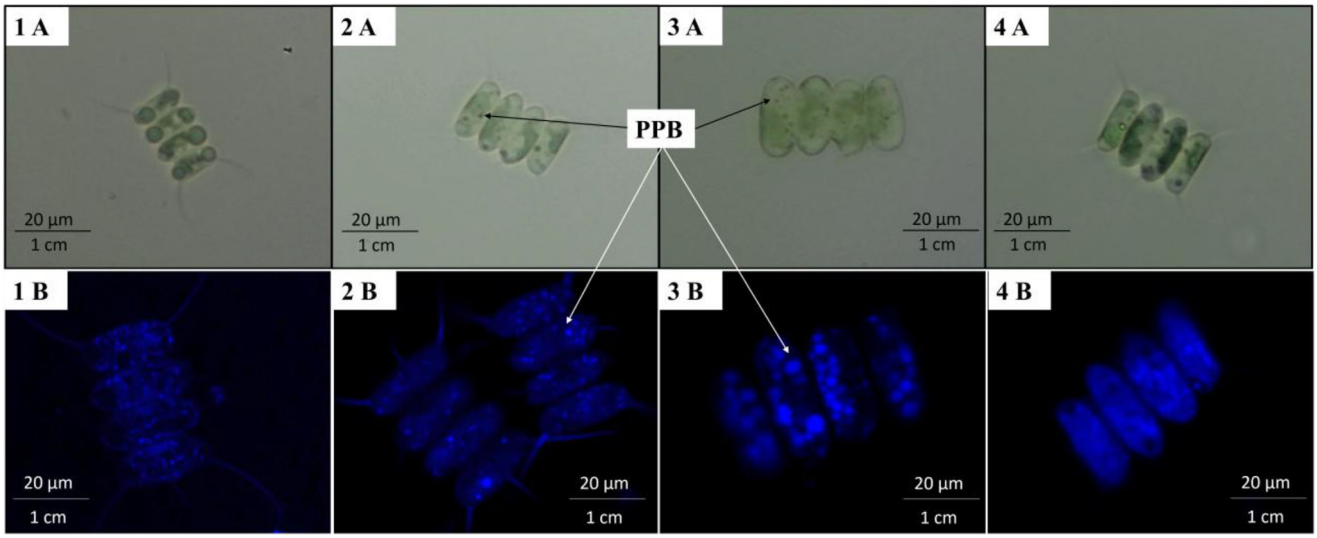


**Figure 2.** A) Light microscopy images at 40x magnification of starved and P refed cells after specific time intervals B) Similar cells viewed under fluorescence microscopy after DAPI staining. (1) Starved cells; (2) 1 min after P addition; (3) 6 h after P addition; (4) 24 h after P addition.

of PLA having more total phosphorus than our biomass. Our results showed that biocomposites of boosted microalgae had superior properties compared to all the other biocomposites and the properties improve with an increase in biomass weight content. While these findings established the potential of microalgae as a sustainable additive, the underlying mechanisms of phosphorus uptake and storage remained unclear, limiting further optimization.

This study takes a more controlled and mechanistic approach to phosphorus enrichment by examining biomass at different time points during the starvation and refeeding process. Our results reveal that luxury phosphorus uptake follows a triphasic system, challenging the previously suggested biphasic model. By systematically analyzing biomass composition throughout these phases, we identify optimal conditions for maximizing P recovery and improving biocomposite performance.

To assess the impact of internal phosphorus levels, standardized weight percentages of biomass from different uptake phases are compounded into PLA. Various physical and chemical properties are tested, with a particular focus on flame retardancy. The findings indicate that specific stages of phosphorus enrichment lead to superior material properties, offering a more targeted strategy for developing high-performance, sustainable biocomposites. This work provides new insights into phosphorus metabolism in microalgae and its direct influence on biocomposite functionality, paving the way for further advancements in circular economy applications.

## 2. Results and Discussions

### 2.1. Biomass Productivity and ww Treatment Efficiency

**Figure 1** illustrates the outcomes of the batch phase growth conducted at the pilot scale to prepare the photobioreactor for continuous phase operations.[12] During the batch phase, 1000 liters of synthetic AnMBR ww containing 160 mg $L^{-1}$ of TN and 10 mg $L^{-1}$ of TP were treated within 11 days. By the end of the treatment, TN and TP levels were reduced to less than 0.02 mg $L^{-1}$, representing a 99% removal rate, far below the European discharge requirements of 10–15 mgN $L^{-1}$ and 1–2 mgP $L^{-1}$, or a minimum reduction of 70–80% for nitrogen and 80% for phosphorus.[13] The average biomass productivity achieved was 0.102 g $L^{-1}$ $day^{-1}$, with maximum biomass concentrations reaching 1.2 g $L^{-1}$ and a peak specific growth rate of 0.25. The average TN and TP removal rates were 14.54 and 0.91 mg $L^{-1}$ $day^{-1}$, respectively, with a ww treatment efficiency of ≈91 liters $day^{-1}$.

Following the transition to continuous phase operations, TN and TP levels in the clean effluent consistently remained below 0.02 mg $L^{-1}$.[14] **Table 1** presents a comparison of the efficiencies achieved during batch versus continuous phase operations. During the continuous phase, 99.9% of TN and TP were removed from the ww, with purification efficiency ranging from 250 to 400 liters per day, improving with increased sunlight. The minimum TN and TP removal rates were 37.5 and 2.5, respectively, representing increases of 158% and 175% over batch phase values. The maximum removal rates achieved were 60 and 4 mg $L^{-1}$ $day^{-1}$, respectively, which are 313% and 309% higher than the batch phase values. The average biomass productivity during continuous operations was 0.43 g $L^{-1}$ $day^{-1}$, a 322% improvement over batch phase productivity, while maintaining a maximum biomass concentration of 0.95 g $L^{-1}$ and achieving average specific growth rates between 0.25 and 0.40, which also increased with available sunlight. The increased performance during continuous cultivation can be attributed to prolonged retention time (RT) and high nutrient load while maintaining favorable conditions.[15]

### 2.2. P enrichment of Starved Cells and Microscopic Confirmation

The cells produced were stored daily under transient light (<100 µE $m^{-2}$ $s^{-1}$) in phosphorus starvation conditions (TN = 16 mg $L^{-1}$, TP = untraceable) to induce the complete consumption of

**Table 2.** Major elements (N, P, and C) content in microalgae biomass. TN stands for total Nitrogen and TP stands for total Phosphorus and C is the carbon content in the biomass. Total volume 1000L.

| | TN removed from WW (±1) (g) | % N in Biomass (±1) | TN in Biomass (±5) ($g\ day^{-1}$) | N uptake rate ($g\ h^{-1}$) | % N Recovered (±0.5) | TP removed from WW (±0.1) (g) | % P in Biomass (±0.1) | TP in Biomass (±0.2) (g) | P uptake rate ($g\ h^{-1}$) | % P Recovered (±0.1) | C in Biomass (±0.15) (%) |
|---|---|---|---|---|---|---|---|---|---|---|---|
| Regular | 102.40 | 18.00 | 91.80 | 3.60 | 89.65 | 6 | 1.10 | 5.61 | 0.24 | 91.77 | 55.11 |
| Starved (per day) | 118.40 | 10.00 | 43.00 | - | 36.32 | 6 | 0.80 | 3.44 | - | 57.33 | 53.21 |
| P+(2 h) | 2.82 | 12.60 | 54.18 | 5.59 | 51.49 | 0.19 | 0.88 | 3.79 | 0.35 | 59.59 | 54.72 |
| P+(4 h) | 16.21 | 16.69 | 71.77 | 8.80 | 60.50 | 1.01 | 1.10 | 4.73 | 0.94 | 64.79 | 53.19 |
| P+(6 h) | 29.11 | 19.73 | 84.84 | 6.55 | 64.51 | 1.82 | 1.33 | 5.72 | 0.99 | 68.83 | 53.11 |
| P+(8 h) | 33.72 | 21.60 | 92.88 | 4.02 | 68.23 | 2.11 | 1.31 | 5.63 | –0.09 | 67.67 | 54.26 |
| P+(10 h) | 38.30 | 24.32 | 104.58 | 5.85 | 74.33 | 2.33 | 1.30 | 5.60 | 0.03 | 67.23 | 55.21 |

intracellular phosphorus reserves. **Figure** 2A (1-4) depicts light microscopy images taken at various stages, from starvation to up to 24 h after phosphorus reintroduction. In Figure 2(1A), cells that had been starved for 10 days and then exposed to light appear small, flattened, and lack granular formations. After just one minute of reintroducing phosphorus, the cells begin to exhibit granular "objects" (2A). These objects have been identified in other microalgae species as acid-insoluble polyphosphate bodies (PPB) accumulated through luxury phosphorus uptake (LPU).[7] After 6 and 12 h of exposure to phosphorus and nitrogen-rich environments under light at pH 7.8, the cells appear larger and more robust, with numerous PPB bodies visible (3A and 4A).

To confirm that these granules are PPB bodies, fluorescence microscopy with (4',6-diamidino-2-phenylindole) DAPI staining was performed, as shown in Figure 2B (1-4). Fluorescence microscopy of the starved cells reveals that DAPI weakly binds to phosphorus on the cell walls with very weak internal response (1B). After one minute of phosphorus reintroduction, DAPI strongly binds to the granular bodies inside the cells and appear as darker stained spots that fluoresce brightly (2B). As the cells become healthier and more robust, focusing the entire cell in a single plane becomes challenging due to the increased sphericity of the cells and granules. After 6 h of LPU, a clear accumulation of PPB bodies is visible (3B). By 24 h, the inorganic intracellular PPB bodies appear to be assimilated, with a much stronger DAPI reaction on the cell walls, suggesting a possible conversion to cell membrane phospholipids (4B). Cells were harvested at various stages for further analysis: immediately after continuous cultivation (regular cells), after a 10-day starvation period (starved cells), and at intervals of 2, 4, 6, 8, and 10 h following phosphorus enrichment (P-enriched cells).

### 2.3. Element Analysis and Mass Balance

**Table** 2 presents the average content of nitrogen (N), phosphorus (P), and carbon (C) in the algae biomass, based on triplicate measurements taken from various locations within the reactor or storage containers during regular continuous cultivation, post-starvation, and following phosphorus reintroduction. After the biomass was generated during the continuous cultivation phase and before they are stored in cubic containers for starvation, the biomass contained 18% N and 1.1% P (average), while the cell content was 410 g in the 1000 L culture. After the starvation period, the N and P content decreased to 10% and 0.8% (average), respectively, and the cell content was at 430 g in the same volume. However, upon reintroducing nutrients, the N and P content in the biomass increased significantly, reaching maximum levels of 18.67% and 1.33% (average) respectively, just 10 h after nutrient reintroduction. These values are consistent with those reported in the literature for similar species, which show N content ranging from 6% to 25% and P content from 0.5% to 1.5%.[12,14] However, the highest internal P levels reached by the biomass was 1.33% and this was achieved 6 h after reintroduction of fresh media. Between 6 and 10 h, the P levels seem to have remained constant with some of it even being released back into the media, which is also something that microalgae are known to do

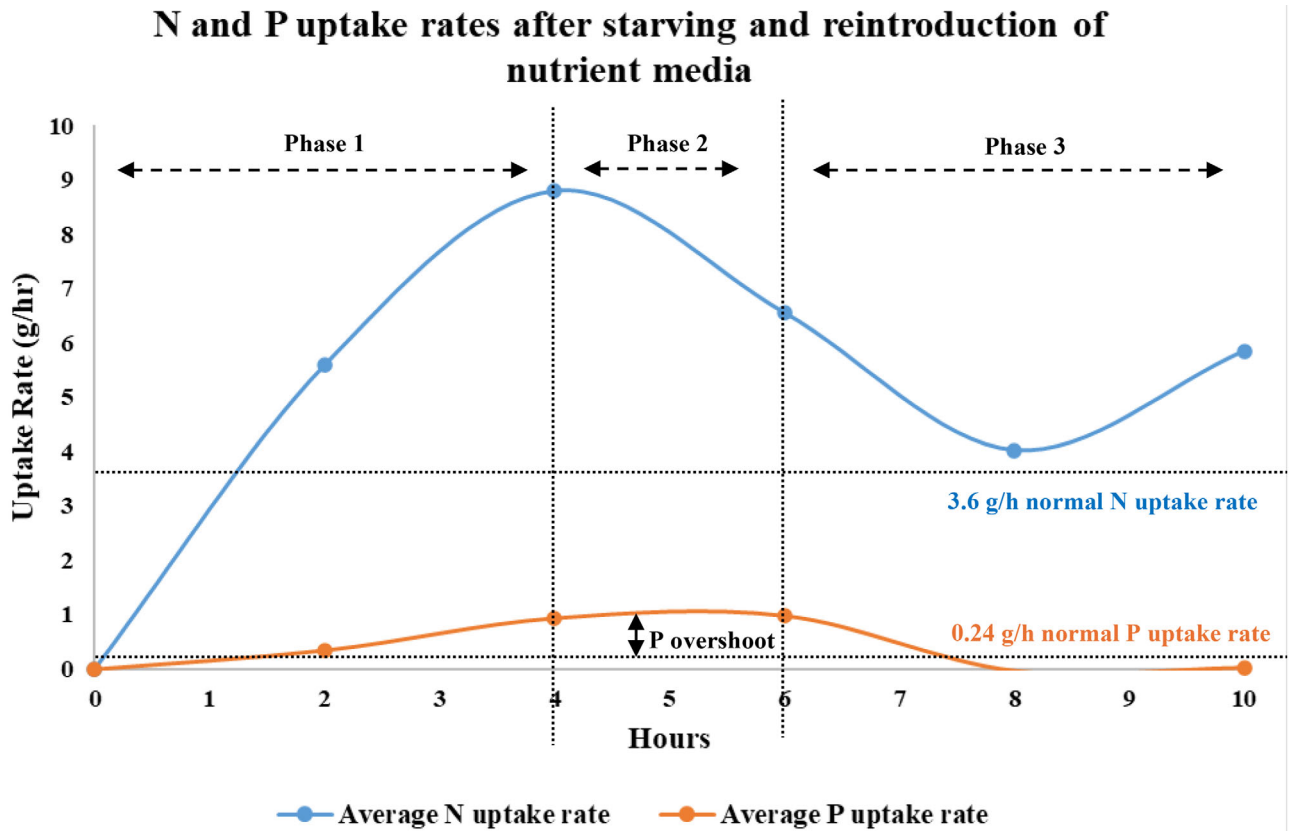


**Figure 3.** Comparison of N and P uptake rates of the biomass every hour after starving and reintroduction of nutrient-rich media and with the uptake rates of normally cultivated (regular continuous cultivation) biomass.

under unfavorable conditions giving us a negative P uptake rate between 6 and 8 h.[16]

**Figure 3** shows the N and P uptake rates of the biomass after they had been starved and reintroduced into nutrient media. It can be seen that the N and P uptake rates during the boosting phase right after starvation seem to be much higher than the rates observed during regular continuous cultivations. This phenomenon has also been reported before and is aptly termed as "hyper-compensation" or "phosphate overplus."[17] During the boosting phase, we can observe a triphasic kinetic in the $P_i$ uptake. The first 2 h or so, the N and P uptake rates gradually increase reaching a maximum of 8.8 g $h^{-1}$ for N and 0.94 g $h^{-1}$ for P. This (fast) uptake in the second stage continues till 6 h or so after the reintroduction of nutrient-rich media along with no growth in cell numbers. Between the 8th and 10th hours, N uptake continues at a reduced rate. This likely reflects the utilization of nitrogen for phospholipid production.[18] Concurrently, cell division commences, and we observe a decrease in phosphorus storage as polyphosphate bodies (PPB) and total cellular phosphorus decline. This marks the onset of the third phase. Our results are in slight contradiction to what has been observed in similar trials where they report only a biphasic system of fast P uptake for the initial few hours followed by slow P uptake.[17,19]

For regular continuous cultivated cells, ≈90% of the TN and 92% of the TP added to the system were recovered. A minor loss of 8–10% of nutrients due to biofilm formation was noted, which can lead to an underestimation of N and P recovery. To mitigate such losses, preventive measures like hydrophobic coatings or shading during summer months could be implemented.

**Table 3.** Summary of the decomposition steps observed for PLA and its algal biocomposites. $T_{5\%}$ represents the temperature at which 5 wt.% of the total mass was lost and $T_{max}$ represents the peak mass loss temperature.

| Sample | $T_{5\%}$ [°C] | $T_{max}$ [°C] | $ML_{max}$ [wt.%] | Residue (800 °C) [wt.%] | |
|---|---|---|---|---|---|
| | | | | Measured | Calculated |
| PLA | 341.8 ± 0.6 | 370.8 ± 0.7 | 98.8 ± 0.1 | 1.2 ± 0.1 | 0 |
| PLA_$P_{0.8}$-Alage$_{20\%}$ | 315.3 ± 1.0 | 362.2 ± 0.1 | 94.9 ± 0.6 | 5.1 ± 0.6 | 5.2 |
| PLA_$P_{1.1}$-Alage$_{20\%}$ | 295.5 ± 0.3 | 347.0 ± 0.4 | 91.5 ± 0.1 | 8.5 ± 0.1 | 5.2 |
| PLA_$P_{1.33}$-Alage$_{20\%}$ | 314.1 ± 0.1 | 357.2 ± 0.1 | 96.7 ± 0.5 | 3.3 ± 0.5 | 5.2 |

During the starvation phase, there was a notable reduction in biomass N and P content, accompanied by ≈15% reduction in biomass weight. If cells from this phase are used, only ≈36% of total N and 57% of total P from the treated ww are recovered. However, six hours after the reintroduction of fresh ww, N and P recovery rates improved to ≈ 65% and 69%, respectively. On continued exposure to the nutrient media, nitrogen recovery rates seem to keep improving reaching almost 75%, however, the P recovery rates seem to be maximum at the 6 h mark with the highest amount of internal P accounting for 1.33% of the total biomass making this an optimal time for harvesting microalgae cells as the P content reduces over the next couple of hours. This timeline is also consistent with other similar works with different species where PPB content peaked 6 h after refeeding of the starved culture with nutrient rich media.[19] Throughout all stages, the average TN and TP levels in the clean effluent of the photobioreactor (PBR) were below detection limits, indicating efficient nutrient recovery. Despite this, the remaining ww after harvesting phosphorus-enriched cells still contained high levels of N and P, preventing direct discharge. This ww was reused to boost starved cells or during continuous cultivation.

The carbon content in the algal biomass remained consistently stable, exceeding 50% throughout the experiment. A small amount of $Na_2CO_3$ (0.2 g $L^{-1}$, contributing 22.6 mg $L^{-1}$ of carbon) was added to the synthetic AnMBR effluent to regulate pH, but its effect on biomass carbon was negligible. On average, under our setup and operating conditions, producing 1 kg of dry biomass captures ≈1.8 kg of $CO_2$ from the atmosphere. Given an average biomass yield of 0.433 g $L^{-1}$ per day, a one-hectare facility with a photobioreactor (PBR) capacity of 500000 L could sequester ≈390 kg of $CO_2$ daily.

### 2.4. Pyrolysis

Thermogravimetric analysis (TGA) was performed under inert conditions to examine the pyrolysis behavior of the biocomposites, with data presented in **Table 3** and **Figure 4A**. Table 3 outlines the decomposition stages observed for PLA and its algae-based biocomposites. The onset of thermal decomposition was identified by the temperature at which 5 wt.% mass loss occurred (T5%), while the peak mass loss temperature ($T_{max}$) indicated the characteristic decomposition temperature. Figure 4A illustrates the thermal decomposition profiles and mass loss rates of biocomposites containing 20 wt.% of various microalgae fillers, including starved algae, regularly grown algae, and phosphorus-enriched algae (enriched over 6 h). Results show that the incorporation of different algae fillers influences the thermal stability of PLA. Pure PLA decomposes at 370 °C, but the addition of algae fillers reduces both T5% and $T_{max}$, leading to an earlier onset of decomposition (Figure 4A). Specifically, PLA with 0.8 wt.% phosphorus-enriched algae (P-Algae) exhibited a decomposition peak 4 °C earlier, with the temperature drop reaching up to 54 °C as the P-Algae content increased. These findings are consistent with other industrial PLA fillers like P-Lignin and Zinc phytate.[11] The biocomposite with regularly grown algae showed

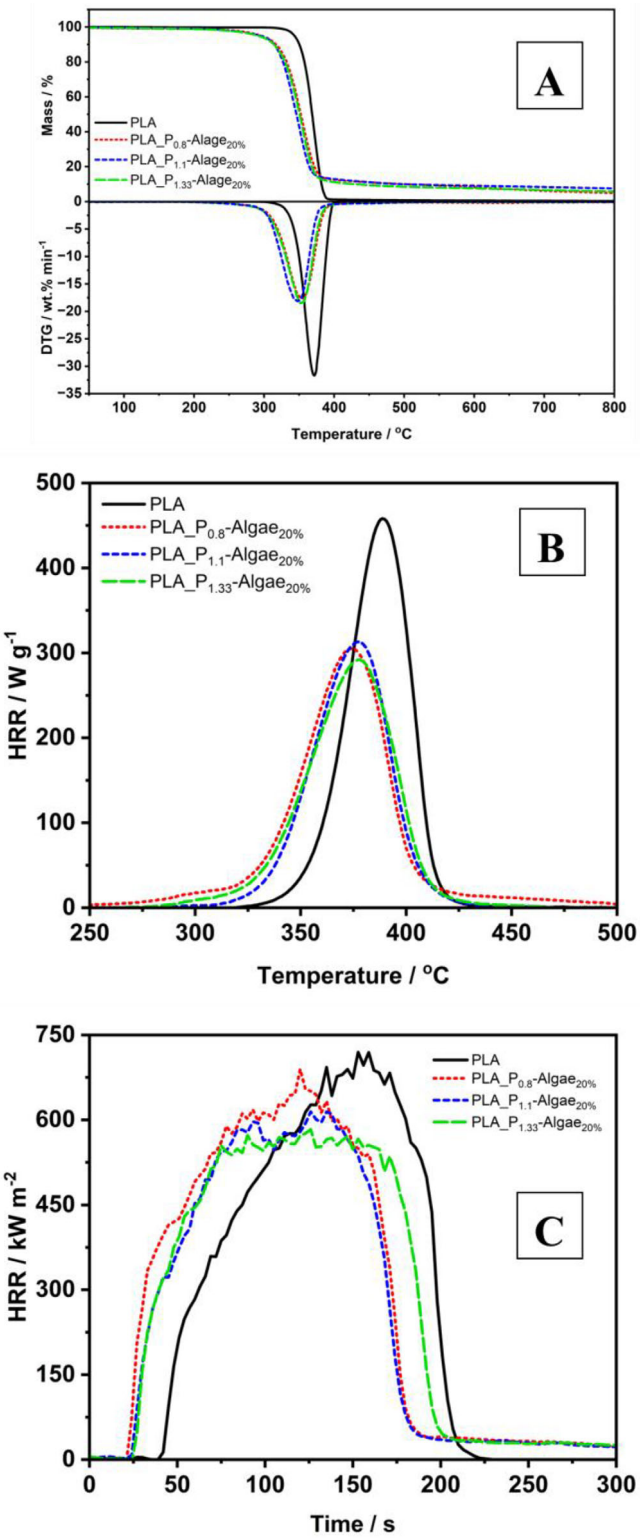


**Figure 4.** A) TGA: Mass and DTG curves, B) PCFC: Heat release rate curve, and C) Cone calorimeter: HRR for PLA and 20 wt.% microalgae filler composites with 0.8%(starved), 1.1%(regular) and 1.33%(enriched) total phosphorus in the biomass by weight.

the most pronounced decrease in decomposition temperature, suggesting that these algae reduce the thermal stability of the PLA matrix. This reduced stability is likely due to phospholipids produced by the algae when exposed to high nitrogen and phosphorus levels, which bond with PLA polymers and lower thermal resistance.[11,20] In contrast, phosphorus-enriched algae outperformed starved cells, reflecting their higher internal phosphorus content, a trend also observed in related studies.[11]

To evaluate parameters such as Heat Release Capacity (HRC) and Total Heat Evolved (THE), normalized by mass to assess flammability, pyrolysis combustion flow calorimetry (PCFC) was used, with data shown in **Table 4** and Figure 4B. It was observed that HRC values were lower for all tested materials compared to PLA, with the best results achieved in the composite containing phosphorus-enriched algae, showing a 38% decrease in HRC. This indicates that even small amounts of absorbed phosphorus in algae enhance flame-retardant properties. Biocomposites with both regular and enriched algae showed similar reductions in THE, surpassing both PLA and the starved algae composite. $T_{max}$ remained similar across all tested biocomposites. Overall, small variations in the phosphorus content absorbed by the algae did not significantly affect decomposition temperature or rate during TGA but did impact other thermal behavior of the biocomposites. In PCFC measurements, the residual mass after pyrolysis was consistent across the biocomposites.

### 2.5. Fire Behavior

Cone calorimeter tests provided detailed insights into the fire behavior of PLA-based biocomposites under forced flaming conditions, with an analysis focused on key parameters such as Peak Heat Release Rate (pHRR), Total Heat Evolved (THE), apparent Effective Heat of Combustion (EHC), and Maximum Average Rate of Heat Emission (MARHE), as presented in **Table 5**. Figure 4C illustrates the HRR results for PLA and its biocomposites with different algae fillers at a concentration of 20 wt.%. The addition of fillers reduced the time to ignition compared to PLA, likely due to earlier decomposition and changes in heat absorption and thermal conductivity in the molten layer.[11,21] This earlier decomposition was also observed in TGA and PCFC measurements in Figure 3A,B. The reduction in the maximum heat release rate, along with a broader release curve, corresponds to these observed thermal changes.

The most notable change in flame behavior occurred with the 20 wt.% phosphorus-enriched algae (1.33%-P) composites, which had a lower pHRR than PLA and the other biocomposites. This pHRR reduction is attributed to charring, which forms a protective layer. The starved algae (0.8%-P) composite burned intensely but extinguished quickly, consuming all available fuel, whereas the regular (1.1%-P) and phosphorus-enriched composites burned more slowly and with less intensity. Fire load analysis showed that the phosphorus-enriched samples released less heat over a longer period, while the starved samples had the highest and quickest heat release. The improved flame retardancy in the phosphorus-enriched composite is likely due to the gradual release of phosphorus compounds from the decomposing algae cells, which may scavenge radicals and enhance heat insulation through a carbonaceous char layer.[22] PLA loaded with microalgae showed improved fire performance, with the 20 wt.% phosphorus-enriched algae composite achieving the most significant reduction in pHRR—≈20% lower than PLA. For this composite, the HRR curves plateaued, with the peak disappearing entirely.

THE corresponds to the overall fire load: lower THE indicates reduced fire hazards and less energy emitted to the environment. All PLA/algae composites exhibited similar fire loads, with the lowest observed in the sample containing regular algae. Unlike pure PLA, which left no residue after testing, all biocomposites produced a comparable amount of char. However, the protective layer created by the algae was not homogeneous and did not fully cover the specimen's surface, suggesting that, as noted in previous research, combustion interruption primarily occurs in the gas phase.[11]

Total Smoke Production (TSP) was higher in composites containing more phosphorus, though TSP values remained low, only slightly above that of pure PLA due to the algae addition. MARHE, an index summarizing flame spread, was higher in biocomposites compared to pure PLA and decreased as the phosphorus content in the algae increased. The cone calorimeter fire behavior results showed similar performance for the starved and regular algae cell biocomposites, highlighting the effectiveness of phosphorus-enriched algae as a sustainable flame retardant for PLA.

Owing to the improved flame retardant properties, the biocomposite has a variety of applications as technical polymers in sectors where flame retardancy is demanded, such as materials for railway vehicles in transportation, housings in electrical engineering, or building materials in construction.

## 3. Conclusion

This study highlights the effective utilization of microalgae and a standardized "feast-famine" protocol for recovering nitrogen (N) and phosphorus (P) from ww and using it to enhance the properties of PLA-based biocomposites. Regularly growing cells demonstrated high nutrient recovery rates, though biofilm formation led to minor losses. Starving the algae reduced N and P content and cell concentration, but nutrient reintroduction quickly restored and improved these levels by "hyper-compensation". Phosphate accumulation and PPB formation follow a triphasic process. In the first phase, cells take ≈2 h to slowly start accumulating nitrogen (N) and phosphorus (P). The second phase involves rapid phosphorus uptake, which lasts until 6 h. Afterward, the uptake slows but continues at this reduced rate. During this time, inorganic PPB is gradually assimilated into the cells. It is no longer available as free inorganic phosphorus, becoming part of phospholipids and nucleic acids instead.

The carbon content in the algal biomass remained stable, contributing significantly to atmospheric $CO_2$ sequestration. The algae's efficient nutrient uptake and $CO_2$ sequestration underscore its environmental benefits in ww treatment and bio-based material production. Thermogravimetric analysis revealed that adding microalgae fillers to PLA affected its thermal stability, with P-enriched cells enhancing performance due to higher internal phosphorus content. The pyrolysis and combustion studies indicated that biocomposites with P-enriched algae exhibited better

**Table 4.** Pyrolysis combustion flow calorimetry (PCFC) results comparing the Heat Release Capacity (HRC) and Total Heat Evolved (THE) between the biocomposites.

| Sample | Residue [wt.%] | HRC [J $gK^{-1}$] | THE [kJ $g^{-1}$] | $T_{max}$ [°C] |
|---|---|---|---|---|
| PLA | 0.4 ± 0.1 | 484 ± 4 | 17.5 ± 0.1 | 389.8 ± 2.1 |
| PLA_$P_{0.8}$-$Alage_{20\%}$ | 6.4 ± 0.1 | 316 ± 12 | 15.9 ± 1.1 | 374.5 ± 4.4 |
| PLA_$P_{1.1}$-$Alage_{20\%}$ | 5.4 ± 0.1 | 318 ± 2 | 14.3 ± 0.1 | 372.1 ± 1.4 |
| PLA_$P_{1.33}$-$Alage_{20\%}$ | 5.3 ± 0.1 | 298 ± 5 | 14.9 ± 0.1 | 373.3 ± 1.0 |

fire retardancy, lower heat release rates, and increased char yield compared to pure PLA.

Overall, the study validates the potential of microalgae as a sustainable additive in biocomposites, enhancing both nutrient recovery from ww and the thermal and fire performance of PLA. This approach supports the development of environmentally friendly materials and strengthens sustainable waste management practices.

Now, let's address whether it makes sense to starve and then boost the biomass, especially when normally growing cells demonstrate much more efficient and reliable nitrogen (N) and phosphorus (P) recovery rates. From an energy perspective, it is more efficient to use the biomass as it is. However, in its current state (without enrichment with inorganic P), the biomass is primarily suitable for use as fertilizer or as a replacement for animal feed. Thus, its usage can be restrictive, especially if the ww used contains high levels of heavy metals and cytotoxins. On the other hand, phosphorus-enriched biomass has broader applications. It can replace various base materials used in production processes, such as inorganic P in traditional flame-retardant materials, thereby reducing the overall need for inorganic P.

In summary, both approaches support sustainability and the circular economy. Regular processes are highly efficient for wastewater treatment and nutrient recovery but have limited applications. Boosted biomass, while slightly less efficient in nutrient recovery, offers greater versatility for broader industrial uses.

## 4. Experimental Section

*Microalgae Species, Growth Medium, and Stock Culture Cultivation*: *Desmodesmus* sp. (KY302863), isolated from a municipal sewage plant in Fulda, Germany was utilized for treating secondary ww.[23] It was a freshwater green microalgae from the family *Scenedesmaceae* and from previous studies in the group had been confirmed to accumulate inorganic P. It was also selected for its high adaptability to German climate conditions and its resilience to nutrient stresses across various ww sources. The primary ww, originating from a potato chip factory in Israel, was initially processed using an anaerobic membrane reactor (AnMBR) at Ben–Gurion University, which effectively removed most of the organic carbon while retaining high phosphorus and nitrogen levels. The composition of the ww was consistent with a lack of micronutrients and maintains a neutral pH between 7 and 7.3. The exact composition of the wastewater can be found in previous works.[24] This specific ww type was chosen because it was a common form of secondary ww in the food industry, which requires nutrients (like N and P) to be removed /recovered prior to discharge, aligning with our goals for a circular economy. Further, the wastewater having already been treated through an Anaerobic membrane reactor, was devoid of harmful or toxic substances like heavy metals and bacteria that could potentially cause problems in upscaling. To simulate this ww as closely as possible, a synthetic version was prepared by adding $NH_4Cl$, $KH_2PO_4$, $MgSO_4$, A5 micro-nutrients, Fe-EDTA, and $Na_2CO_3$ as a pH buffer.[11] Using the synthetic ww, which closely replicated the original AnMBR effluent, eliminated the need for long-distance transport and reduced the risk of chemical alterations during storage.[24] The synthetic ww also ensured consistency and facilitated on-site mass production throughout the experiment. Previous studies with the same microalgal species and ww type showed that pretreating the ww to remove organic carbon was most effective in optimizing the use of hollow fiber systems for microalgae harvesting, by increasing their longevity by reducing fouling.[11] Employing a synthetic version of the WW helped minimize fouling by removing organic carbon.

Stock cultures of *Desmodesmus* sp., maintained in Bold's Basal Medium, were grown in triplicate in 2 L bottle photobioreactors (PBRs) (9 cm in diameter, 15 cm filling height) using the synthetic AnMBR medium to acclimate the cultures to the media in preparation for scale-up. These cultures were maintained at 24 ± 1 °C and illuminated by fluorescent tube lights (L 58W/840, OSRAM, Germany) at 200 µE $m^{-2}$ $s^{-1}$ (measured at the bottle surface closest to the light source) under a 14:10 h light: dark cycle. The pH was controlled between 7.0 and 8.1 through $CO_2$ injection, with continuous aeration provided by an aquarium air compressor (LA-120-A1108-P3-1413, Nitto Kohki, Germany). Initial concentrations of ammonium nitrogen ($NH^{4+}$ -N) and TP in the synthetic AnMBR effluent were 147 mg N $L^{-1}$ and 9.8 mg P $L^{-1}$, respectively.

A 10 L culture was then used to inoculate three 40 L phytobag photobioreactors, developed by Phytolutions GmbH (with patented IP rights), which served as the starter cultures for the pilot plant. The pilot setup provided a continuous air supply at 30 L $min^{-1}$ through tubing and was illuminated by 58 W fluorescent lamps (Osram, Munich, Germany) at 75 µE $m^{-2}$ $s^{-1}$.

*Measurement of Dry Biomass, Optical Density, and Nutrient Concentrations*: Dry biomass concentration was determined using gravimetric methods. Samples (3 mL) were filtered through pre-weighed GF/F filters, which had been pre-washed with deionized (DI) water and dried at 60 °C

**Table 5.** Cone calorimeter results of PLA and its biocomposites.

| Sample | $t_{ig}$ [s] | pHRR [kw $m^{-2}$] | THE [MJ $m^{-2}$] | EHC [MJ $Kg^{-1}$] | RESIDUE [wt.%] | TSP [$m^2$] | MARHE [kW $m^{-2}$] |
|---|---|---|---|---|---|---|---|
| PLA | 39 ± 1 | 736 ± 23 | 81.5 ± 0.5 | 17.6 ± 0.1 | 0 ± 0 | 0. ± 0.1 | 406 ± 2 |
| PLA_$P_{0.8}$-$Alage_{20\%}$ | 20 ± 1 | 661 ± 6 | 79.5 ± 0.2 | 18.0 ± 0.1 | 5.2 ± 0.4 | 1.3 ± 0.7 | 447 ± 3 |
| PLA_$P_{1.1}$-$Alage_{20\%}$ | 26 ± 4 | 651 ± 8 | 72.1 ± 0.3 | 18.2 ± 0.1 | 4.4 ± 0.8 | 1.6 ± 0.2 | 424 ± 3 |
| PLA_$P_{1.33}$-$Alage_{20\%}$ | 23 ± 1 | 591 ± 2 | 78.7 ± 1.3 | 17.8 ± 0.1 | 5.1 ± 0.1 | 2.6 ± 0.4 | 420 ± 1 |

overnight. After filtering the algae samples, the filters were again dried overnight at 60 °C and then weighed using a fine balance. The difference in the filter weights before and after filtering the biomass was used to calculate the dry biomass weight per Liter. To measure nutrient concentrations, algae-free media filtrate was obtained by filtering the samples through a 0.2 µm cellulose acetate filter. The filtrate samples were then diluted with DI water and analyzed according to the instructions provided with the respective kits for $NH^{4+}$-N and TP (LCK 305 and LCK 349, Hach, Germany). The concentrations of $NH^{4+}$-N and TP were measured and recorded using a spectrophotometer (Hach, DR 2800, Germany). Optical density was tracked at 750 nm using a spectrophotometer (6320D, Jenway, UK). The uptake rates for TN and TP, denoted as $P_x$, were calculated using Equation (1), where $c_i$ represents the initial concentration and $c_f$ the final concentration of nitrogen or phosphorus (mg $L^{-1}$) over a growth cycle of $\Delta t_c$ (the time taken for $c_i$ to reach $c_f$). The ww purification rate ($P_w$) was determined using Equation (2), where $V_w$ represents the total volume of ww treated during the growth cycle of $\Delta t_c$. Volumetric biomass productivity ($P_b$) was calculated using Equation (3), where $W_b$ is the dry biomass produced (grams) during a growth cycle of $\Delta t_c$, with V representing the total bioreactor capacity in Liters.

$$P_x = \frac{c_f - c_i}{\Delta t_c} \tag{1}$$

$$P_w = \frac{V_w}{\Delta t_c} \tag{2}$$

$$P_b = \frac{W_b}{\Delta t_c V} \tag{3}$$

*Photobioreactor*: The photobioreactor (PBR) consisted of four main components, as detailed in a previous study.[25] The setup included five specially designed polyethylene (PE) phytobags, each measuring 5 meters in length and 1.5 meters in height, with a volume of 200 liters. These phytobags were connected to a circulation system operated by a peristaltic pump (Axflow, London, United Kingdom). To maintain the temperature between 18 and 24 °C, optimal for the growth of *Desmodesmus* sp., a heat exchange system was incorporated into the circulation setup, allowing for production in both winter and summer. Aeration was provided by an air pump linked to micro-bubble air tubes positioned at the bottom of each PE bag. Carbon dioxide was supplied for pH control via an automatic valve, which activated when the pH of the algal solution exceeded 7.8, as detected by a pH sensor. Additionally, a turbidity sensor within the PBR was connected to the harvester for real-time monitoring of cell densities. To ensure a consistent reactor volume during continuous cultivation, a water level sensor in one of the reactors was connected to a pump that added fresh synthetic media when the volume dropped below a preset level. The N and P levels of the ww was regularly monitored. The pilot plant was situated in a greenhouse at the OceanLab facility of Constructor University Bremen, Germany, located at 8°39′1″ E and 53°9′53″ N, where it operated under natural environmental conditions. Consequently, variables such as light and temperature within the PBR fluctuated regularly in response to seasonal changes. *Desmodesmus* sp. was batch cultivated to a volume of 1000 liters during June (summer), with growth kinetics monitored daily. The photobioreactor was connected to a membrane harvesting system that was capable of harvesting the biomass from the PBR along with the treated ww. It then concentrated the cell concentration by removing clean effluent out of the system while retaining the biomass. The biomass can then be removed or sent back into the PBR. Similarly, the clean effluent can be removed from the system or sent back into the PBR for further treatment.[14,26,27]

*Biomass Generation and Phosphorus Enrichment*: Once the bioreactor reached the stationary phase and all nutrients in the media were depleted, confirmed by measuring N and P levels both inside the biomass and in the remaining ww. Continuous cultivation with synthetic ww (WW) was initiated. The dilution rate was kept constant (and equal to the growth rate), ranging between 0.25 and 0.4, depending on the available natural sunlight, using a membrane photobioreactor.[14] Basically, a lower dilution rate was used along with a lower concentration of biomass in the photobioreactor on days with lower levels of sunshine (due to cloud cover) and on days with high levels of sunshine, higher dilution rates and a higher concentration of biomass was used. Sunlight intensity was measured at various points on the PBR's surface throughout the day, and a mini-PAM analyzer (Walz MINI-PAM-II) was used to calculate the average light intensity received during daylight hours. Continuous cultivation was conducted daily for 12 h during daylight, after which the PBR was kept in darkness for the remaining 12 h, with aeration, pH, and temperature still regulated as mentioned before. The biomass generated was concentrated through the day using the membrane photobioreactor and was collected in a cubic container. This allows for more biomass to be stored in a less area footprint.[14,26,27] The biomass was stored in the dark at 4 °C. The pH of the stored biomass was maintained at 7.8, while nitrogen (N) and phosphorus (P) levels were undetectable (<0.05 mg $L^{-1}$) in the media. Before the force starvation, the biomass was slowly returned to room temperature while pH was still maintained between 7 and 7.8. According to our batch phase results, it was estimated that the N:P consumption ratio was 16:1, and the TP content of the biomass was estimated to be ≈1 mg $L^{-1}$. In order to deplete internal phosphorus reserves, $NH_4Cl$ was added to the stored culture to reach a TN concentration of 16 mg $L^{-1}$, as phosphorus consumption by microalgae was intricately linked to nitrogen uptake.[11] The stored biomass was deprived of phosphorus and direct sunlight (<100 µE $m^{-2}$ $s^{-1}$) for 10 days. In other works, studying similar effects in varied species has suggested that 10 days of starvation was optimal for reaching the lowest internal phosphorus reserves also the cell division came to a halt indicating the absence of internal and external P.[18] After these 10 days of starvation, N and P levels were measured both inside the biomass and in the remaining ww. The cubic container was exposed to natural sunlight, and an equal volume of WW was added to the stored biomass, having a nutrient load and cell concentration in the final culture, half of that of the original growth media. This was done to ensure more light penetration and have an effluent with a lower nutrient load in the end and to have a higher rate of ww purification. It has already been established that the rate of phosphorus uptake was not affected by the amount of P in the environment but rather by an abrupt change from low-P to ample-P conditions.[16] The P boosted biomass was harvested using an industrial centrifuge (Delaval, Germany) and then frozen. Samples were taken and frozen before and after the starvation period. The frozen samples were lyophilized at -50 °C under vacuum (Christ Alpha 1–2 LD) to remove intracellular moisture in preparation for further analysis. Additionally, liquid/lyophilized microalgae and WW samples were collected before starvation, after 10 days of starvation, and at intervals of 1 min, 2, 4, 6, 8, and 24 h after reintroducing the media, and then analyzed.

*Microscopy*: Cells were examined under light microscopy to observe changes following phosphorus (P) starvation and after the reintroduction of excess P at intervals of 1 min, 2, 4, 6, and 24 h (Carl Zeiss Axiostar) at 40x magnification. The sensitivity of light microscopy for detecting these changes was validated using epifluorescence microscopy on cell suspensions stained with 4′,6-diamidino-2-phenylindole dihydrochloride (DAPI) using a method previously shown to be effective in discriminating DAPI bonded with DNA and inorganic P.[28] A 100 µL sample of the microalgae culture was fixed on a slide by airdrying, followed by the addition of DAPI (20 µg $ml^{-1}$). DAPI-stained polyphosphate granules emit yellow fluorescence at 526 nm under UV excitation, using a method previously demonstrated to be effective for identifying and staining polyphosphate bodies.[7] Fluorescence images were captured using a Laser Scanning Microscope 980 (ZEISS, Oberkochen, Germany), with the images edited and visualized using PC software (ZEN blue, 3.2.0). The microscope was operated in Airyscan Super Resolution mode with the pinhole set to 5 AU, using an excitation wavelength of 405 nm and a detection range of 499–549 and 673-629 nm.

*Chemical Composition and Mass Balance*: Algae samples were analyzed to assess nutrient recovery at three stages: after starvation, following the formation of polyphosphate (PPB) granules, and from regular cells during the mid-batch phase of cultivation. Key elements, including dissolved organic carbon (DOC), dissolved inorganic carbon (DIC), and TN,

were measured using a TOC analyzer (Multi N/C; Analytik-Jena, Germany) with 5 mg of dry lyophilized biomass. For element concentrations, such as TP, the lyophilized samples were dried at 60 °C for a minimum of 12 h. Aliquots of 50–200 mg were then weighed into acid-cleaned Polytetrafluoroethylene (PTFE) beakers and digested with 25 mL of concentrated $HNO_3$ at 70–90 °C for two hours on a hot plate. The solutions were evaporated, and the process was repeated twice with concentrated HCl, followed by dilution with 25 mL of 0.5 M $HNO_3$. All reagents used were of suprapure grade (Merck, Germany), and deionized (DI) water (18.2 MΩm) was used for diluting the concentrated acids. The sample solutions were filtered through 2 µm cellulose acetate membrane filters using acid-cleaned syringes, further diluted with 0.5 M $HNO_3$, and analyzed using an inductively coupled plasma optical emission spectroscopy (ICP-OES; Spectro Ciros Vision). The certified reference standard BCR-670 was analyzed alongside the algae samples for quality control. Phosphorus concentration of reference materials showed an excellent match with certified references (difference <4% for NIST694) and previously reported values in literature (difference <1.5% for BCR-670). For detailed information on the digestion process, quality control measures, use of internal standards, and instrument settings, refer to previous publications.[29,30] The theoretical nutrient content (eE,X) of the biomass was calculated using Equation (4), based on the initial (cStart) and final (cEnd) concentrations of the nutrient (E) and biomass (X) in g $L^{-1}$ over the specified time interval.

$$e_{E,X} = \frac{c_{E,start} - c_{E,end}}{c_{X,end} - c_{X,start}} \quad (4)$$

*Preparation of Biocomposites*: Biocomposites were created by combining polylactic acid (PLA) (molar mass = $1.47 \times 10^5$ g $mol^{-1}$) with microalgae biomass containing TP levels of 0.8, 1.1, and 1.33 wt.%. Prior to compounding, both the PLA granules and the algae biomass were thoroughly dried overnight in a vacuum oven at 50 °C. The biocomposites were then processed using an Xplore MC 15 HT twin-screw micro-compounder with a 15 mL chamber capacity. Compounding was performed at a rotation speed of 75 rpm, with the temperature set between 190 and 200 °C for a 6-min cycle to ensure a homogeneous mixture. Each biocomposite was formulated with 20 wt.% algae filler.

*Analysis of Biocomposites*: The Pyrolysis Combustion Flow Calorimeter (PCFC) (ASTM D7309, Fire Testing Technologies Ltd, UK) was employed to analyze the volatile products at a constant heating rate of 1 K $s^{-1}$ over a temperature range of 100 to 750 °C. For this analysis, 5 mg of powdered material underwent anaerobic pyrolysis, and the resulting volatile products were combusted at 900 °C in a gas mixture, with a nitrogen flow rate of 80 mL $min^{-1}$ and an oxygen flow rate of 20 mL $min^{-1}$.

Cone calorimeter tests were conducted using a dual cone calorimeter from Fire Testing Technology, UK, which was equipped with a spark igniter, following the ISO 5660 standard. Specimens measuring 100 mm × 100 mm × 4 mm were evaluated in a horizontal orientation under an external heat flux of 50 kW $m^{-2}$. The distance between the cone heater and the sample surface was maintained at 35 mm to accommodate material intumescence without significantly affecting the area of uniform heat flux.[31,32] Each material type was evaluated three times to ensure accuracy. The characterization of the biocomposites in this study primarily focuses on their burning behavior, which directly relate to flame retardant performance. The methods are standardized and based on international norms: PCFC: ASTM D7309, Cone Calorimeter: ISO 5660.

## Acknowledgements

Thanks to the financial support of the Bundesministerium für Bildung und Forschung – BMBF: KMU-innovativ: Bioökonomie 031B1289B.

Open access funding enabled and organized by Projekt DEAL.

## Conflict of Interest

The authors declare no conflict of interest.

## Author Contributions

R.D. was responsible for conceptualization, investigation, visualization, writing the original draft. M.D. contributed to conceptualization, investigation, visualization and writing through review and editing. A.P., T.K. and K.Z. were involved in investigation and data interpretation. C.T. contributed to conceptualization, data interpretation, writing through review and editing, and validation. C.P. were involved in data interpretation, writing through review and editing, and validation. B.S. were involved in conceptualization, data interpretation, writing through review and editing and validation. M.S.U. and L.T. contributed to conceptualization, data interpretation, writing through review and editing and validation.

## Data Availability Statement

The data that support the findings of this study are available from the corresponding author upon reasonable request.

## Keywords

biocomposites, biopolymers, flame-retardant, hyper compensation, phycoremediation, wastewater treatment

Received: March 3, 2025
Published online:

[1] Y. Arora, S. Sharma, V. Sharma, *Arabian Journal for Science and Engineering* **2023**, *48*, 7225.
[2] M. Wang, G.-Z. Yin, Y. Yang, W. Fu, J. L. Díaz Palencia, J. Zhao, N. Wang, Y. Jiang, D.-Y. Wang, *Adv Ind Eng Polym Res.* **2022**, https://doi.org/10.1016/j.aiepr.2022.07.003.
[3] A. Samir, F. H. Ashour, A. A. A. Hakim, M. Bassyouni, *Npj Materials Degradation* **2022**, *6*, 68.
[4] I. van der Veen, J. de Boer, *Chemosphere* **2012**, *88*, 1119.
[5] I. Directorate-General for Internal Market, G. A. Blengini, C. El Latunussa, U. Eynard, C. Torres De Matos, D. Wittmer, K. Georgitzikis, C. Pavel, S. Carrara, L. Mancini, M. Unguru, D. Blagoeva, F. Mathieux, D. Pennington, *Study on the EU's List of Critical Raw Materials 2020: Final Report*, Publications Office Of The European Union, LU **2020**, https://op.europa.eu/en/publication-detail/-/publication/c0d5292a-ee54-11ea-991b-01aa75ed71a1/language-en.
[6] M. M. Velencoso, A. Battig, J. C. Markwart, B. Schartel, F. R. Wurm, *Angew. Chem., Int. Ed.* **2018**, *57*, 10450.
[7] S. Eixler, U. Selig, U. Karsten, *Hydrobiologia* **2005**, *533*, 135.
[8] E. Örtl, Sewage Sludge Disposal in the Federal Republic of Germany **2019**, https://www.umweltbundesamt.de/en/publikationen/sewage-sludge-disposal-in-the-federal-republic-of.
[9] K. Li, Q. Liu, F. Fang, R. Luo, Q. Lu, W. Zhou, S. Huo, P. Cheng, J. Liu, M. Addy, P. Chen, D. Chen, R. Ruan, *Bioresour. Technol.* **2019**, *291*, 121934.
[10] X. Meng, Q. Huang, J. Xu, H. Gao, J. Yan, *Waste Disposal & Sustainable Energy* **2019**, *1*, 99.
[11] M. Dudziak, R. Bhatia, R. Dey, J. Falkenhagen, M. S. Ullrich, C. Thomsen, B. Schartel, *Polym. Degrad. Stab.* **2024**, *227*, 110885.
[12] S. Wang, F. Ortiz Tena, R. Dey, C. Thomsen, C. Steinweg, D. Kraemer, A. D. Grossman, Y. Z. Belete, R. Bernstein, A. Gross, S. Leu, S. Boussiba, L. Thomsen, C. Posten, *Sep. Purif. Technol.* **2022**, *289*, 120744.
[13] bmuv.de. Sewage Sludge Ordinance - BMUV-Laws, https://www.bmuv.de/en/law/sewage-sludge-ordinance (accessed: Febuary 2023).

[14] R. Dey, F. Ortiz Tena, S. Wang, J. Martin Messmann, C. Steinweg, C. Thomsen, C. Posten, S. Leu, M. S. Ullrich, L. Thomsen, *Bioresour. Technol.* **2024**, *391*, 129986.
[15] Y. Liao, P. Fatehi, B. Liao, *Membranes* **2024**, *14*, 245.
[16] M. A. Yaakob, R. M. S. R. Mohamed, A. Al-Gheethi, R. Aswathnarayana Gokare, R. R. Ambati, *Cells* **2021**, *10*, 393.
[17] A. Solovchenko, O. Gorelova, O. Karpova, I. Selyakh, L. Semenova, O. Chivkunova, O. Baulina, E. Vinogradova, T. Pugacheva, P. Scherbakov, S. Vasilieva, A. Lukyanov, E. Lobakova, *Cells* **2020**, *9*, 1933.
[18] L. Guo, Q. Wu, Y. S. Lai, E. Eustance, B. E. Rittmann, *Sci. Total Environ.* **2023**, *858*, 159811.
[19] A. Solovchenko, I. Khozin-Goldberg, I. Selyakh, L. Semenova, T. Ismagulova, A. Lukyanov, I. Mamedov, E. Vinogradova, O. Karpova, I. Konyukhov, S. Vasilieva, P. Mojzes, C. Dijkema, M. Vecherskaya, I. Zvyagin, L. Nedbal, O. Gorelova, *Algal Res.* **2019**, *43*, 101651.
[20] W.-H. Chen, Y.-S. Chu, J.-L. Liu, J.-S. Chang, *Energy Convers. Manage.* **2018**, *160*, 209.
[21] B. Dittrich, K.-A. Wartig, D. Hofmann, R. Mülhaupt, B. Schartel, *Polym. Degrad. Stab.* **2013**, *98*, 1495.
[22] B. Schartel, *Materials* **2010**, *3*, 4710.
[23] J. Han, L. Thomsen, K. Pan, P. Wang, T. Wawilow, O. Osundeko, S. Wang, U. Theilen, C. Thomsen, *Environ. Technol.* **2019**, *42*, 3261.
[24] A. D. Grossman, Y. Z. Belete, S. Boussiba, U. Yogev, C. Posten, F. Ortiz Tena, L. Thomsen, S. Wang, A. Gross, S. Leu, R. Bernstein, *Sci. Total Environ.* **2021**, *779*, 146373.
[25] S. Wang, I. H. Said, C. Thorstenson, C. Thomsen, M. S. Ullrich, N. Kuhnert, L. Thomsen, *Algal Res.* **2018**, *32*, 113.
[26] F. O. Tena, K. Ranglová, D. Kubač, C. Steinweg, C. Thomson, J. Masojidek, C. Posten, *Eng. Life Sci.* **2021**, *21*, 607.
[27] F. O. Tena, V. Bickel, C. Steinweg, C. Posten, *Sci. Total Environ.* **2023**, *912*, 169082.
[28] J. J. Christ, S. Willbold, L. M. Blank, *Anal. Chem.* **2020**, *92*, 4167.
[29] K. Zhang, A.-L. Zocher, M. Bau, *Sci. Total Environ.* **2024**, *958*, 178056.
[30] A.-L. Zocher, F. Klimpel, D. Kraemer, M. Bau, *Appl. Geochem.* **2021**, *134*, 105025.
[31] F. D. Sypaseuth, E. Gallo, S. Çiftci, B. Schartel, *E-Polymers* **2017**, *17*, 449.
[32] B. Schartel, M. Bartholmai, U. Knoll, *Polym. Degrad. Stab.* **2005**, *88*, 540.